BIOCHEMISTRY
including biophysical chemistry & molecular biology

Article

pubs.acs.org/biochemistry

Substrate Orientation and Specificity in Xanthine Oxidase: Crystal Structures of the Enzyme in Complex with Indole-3-acetaldehyde and Guanine

Hongnan Cao,[†] James Hall, and Russ Hille*

Department of Biochemistry, University of California, Riverside, California 92521, United States

ABSTRACT: Xanthine oxidase is a molybdenum-containing hydroxylase that catalyzes the hydroxylation of sp^2-hybridized carbon centers in a variety of aromatic heterocycles as well as aldehydes. Crystal structures of the oxidase form of the bovine enzyme in complex with a poor substrate indole-3-acetaldehyde and the nonsubstrate guanine have been determined, both at a resolution of 1.6 Å. In each structure, a specific and unambiguous orientation of the substrate in the active site is observed in which the hydroxylatable site is oriented away from the active site molybdenum center. The orientation seen with indole-3-acetaldehyde has the substrate positioned with the indole ring rather than the exocyclic aldehyde nearest the molybdenum center, indicating that the substrate must rotate some 30° in the enzyme active site to permit hydroxylation of the aldehyde group (as observed experimentally), accounting for the reduced reactivity of the enzyme toward this substrate. The principal product of hydroxylation of indole-3-acetaldehyde by the bovine enzyme is confirmed to be indole-3-carboxylic acid based on its characteristic UV−vis spectrum, and the kinetics of enzyme reduction are reported. With guanine, the dominant orientation seen crystallographically has the C-8 position that might be hydroxylated pointed away from the active site molybdenum center, in a configuration resembling that seen previously with hypoxanthine (a substrate that is effectively hydroxylated at position 2). The ∼180° reorientation required to permit reaction is sterically prohibited, indicating that substrate (mis)orientation in the active site is a major factor precluding formation of the highly mutagenic 8-hydroxyguanine.

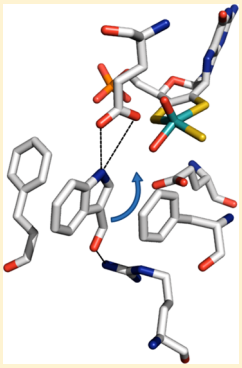

Xanthine oxidase is the eponymous member of a large family of molybdenum-containing enzymes that catalyze the hydroxylation of carbon centers in a broad range of aromatic heterocycles and aldehydes.[1−4] The bovine enzyme has been crystallized and found to be a homodimer, with each subunit containing four redox-active sites in separate, well-defined domains of the polypeptide: an active site molybdenum center, a pair of spinach ferredoxin-like [2Fe-2S] clusters, and FAD.[5] The overall catalytic sequence consists of a reductive half-reaction in which the substrate is oxidatively hydroxylated at the molybdenum center [reducing it from Mo(VI) to Mo(IV)] and, after intramolecular electron transfer involving the intervening Fe−S centers, an oxidative half-reaction in which the reducing equivalents are removed from the enzyme via its FAD (with O_2 and NAD^+ serving as the electron acceptor for the oxidase and dehydrogenase forms of the enzyme, respectively).[1,4] As shown in Figure 1, the oxidized molybdenum center has an $LMo^{VI}OS(OH)$ structure in a square-pyramidal coordination geometry, with the Mo═O group occupying the apical position; L represents the enedithiolate ligand of a pyranopterin cofactor common to all mononuclear molybdenum- and tungsten-containing enzymes. In the reductive half-reaction, substrates are hydroxylated at a specific carbon position in a reaction initiated by nucleophilic attack of the equatorial Mo-OH group of the metal center upon deprotonation involving a conserved glutamate residue (Glu 1261 in the bovine enzyme), as shown in Figure 1.[6,7] Hydride is then transferred from the carbon being hydroxylated to the Mo═S group of the molybdenum coordination sphere, yielding a key intermediate that can be formulated as $LMo^{IV}O(SH)(OR)$, where OR represents the now-hydroxylated product coordinated to molybdenum via the catalytically introduced hydroxyl group.[8−10] The structure of this intermediate has been confirmed by X-ray crystallography of the bovine enzyme in reaction with the slow substrate 2-hydroxy-6-methylpurine.[11] Finally, the bound product is displaced from the molybdenum coordination sphere by solvent hydroxide to regenerate the Mo-OH ligand in preparation for a subsequent catalytic cycle.

Several active site residues are highly conserved in the xanthine-hydroxylating enzymes of many species, including two phenylalanine residues that constrain the bound substrate to a plane perpendicular to the equatorial plane of the molybdenum center, as well as Glu 1261, Glu 802, and Arg 880. Glu 1261 is believed to function as the catalytic base in both the heterocycle- and aldehyde-utilizing molybdenum hydroxylases.[7,12−14] The oxygen atom of the Mo-OH is within hydrogen bonding distance of this glutamate in both the bovine and bacterial enzymes,[5,15] and an E730A variant of the *Rhodobacter capsulatus* enzyme is essentially inactive toward xanthine, conservatively exhibiting an at least 10^7-fold reduction in the limiting rate of enzyme reduction relative to that of the

Received: October 28, 2013
Revised: December 18, 2013
Published: January 3, 2014

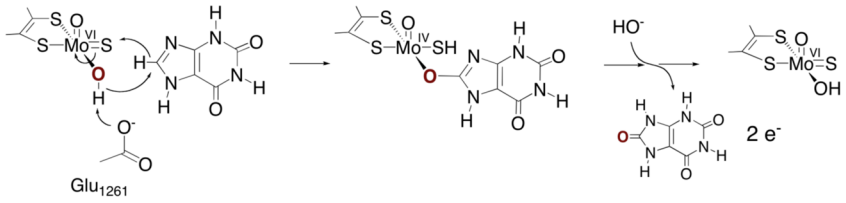

Figure 1. Reaction mechanism for xanthine oxidase. Catalysis is initiated by base-assisted nucleophilic attack of the equatorial Mo-OH on the C-8 atom of xanthine with concomitant hydride transfer from C-8 to Mo=S, resulting in reduction of Mo(VI) to Mo(IV). Reoxidation of the molybdenum center occurs by the transfer of an electron to the other redox-active centers of the enzyme, accompanied by deprotonation of the Mo-SH bond and displacement of the bound product by hydroxide from solvent to regenerate the Mo-OH group.

wild-type enzyme.[6] Arg 880, which is conserved only in the heterocycle-oxidizing enzymes and is usually a methionine in those molybdenum-containing hydroxylases that act on aldehydes, has been proposed to stabilize the accumulation of negative charge on the heterocycle in the course of nucleophilic attack via electrostatic interactions with the C-6 carbonyl oxygen of xanthine.[16] The guanidinium group of this arginine is within hydrogen-bonding distance of the C-6 carbonyl oxygen of xanthine bound at the active site,[17] and its mutation to methionine in the *R. capsulatus* enzyme results in a 2×10^4-fold decrease in the reaction rate with xanthine as the substrate.[16] Comparable results in steady-state experiments have been seen for the homologous mutations of the human enzyme.[18]

We have previously shown that hypoxanthine binds to bovine xanthine oxidase in two different orientations, only one of which is catalytically competent.[19] This illustrates that the substrate can assume alternate orientations in the active site and that this can influence reactivity. Here we report crystal structures for bovine xanthine oxidase in complex with indole-3-acetaldehyde (a poor substrate for the bovine enzyme, but the physiological substrate for the closely related aldehyde oxidase AOX III from *Arabidopsis thaliana*, for which the product carboxylic acid is an important hormone) and guanine (a purine upon which the xanthine oxidase is known not to act effectively), both at 1.6 Å resolution. Consistent with their poor reactivities, we find that both substrates show a dominant orientation in the active site of the enzyme that is catalytically nonproductive. In the case of indole-3-acetaldehyde, a modest, sterically allowed rotation juxtaposes the aldehyde group with the molybdenum center that allows hydroxylation to take place. With guanine, the substrate must rotate approximately 180° to present its 8 position to the active site molybdenum center for hydroxylation, and this rotation is sterically prohibited. The observed nonproductive orientation seen with guanine provides a steric explanation for how the enzyme discriminates against guanine as the substrate, thereby avoiding *in vivo* formation of the highly mutagenic 8-hydroxyguanine.

EXPERIMENTAL PROCEDURES

Materials. Magnetic bases for use with the automated crystallography system at the LRL-CAT beamline of Argonne National Laboratory (Argonne, IL) were obtained from MAR-USA (Evanston, IL). Mounted cryoloops, magnetic cryovials, and crystal growth materials were obtained from Hampton Research (Aliso Viejo, CA). Polyethylene glycol (PEG) 200 and PEG 8000 stock solutions were obtained from Hampton Research. All other chemicals and reagents, including indole-3-acetaldehyde, indole-3-acetate, and guanine, were obtained at the highest quality or purity available from Sigma-Aldrich or Fisher Scientific and used without further purification. The structures of compounds relevant to this work are shown in Figure 2.

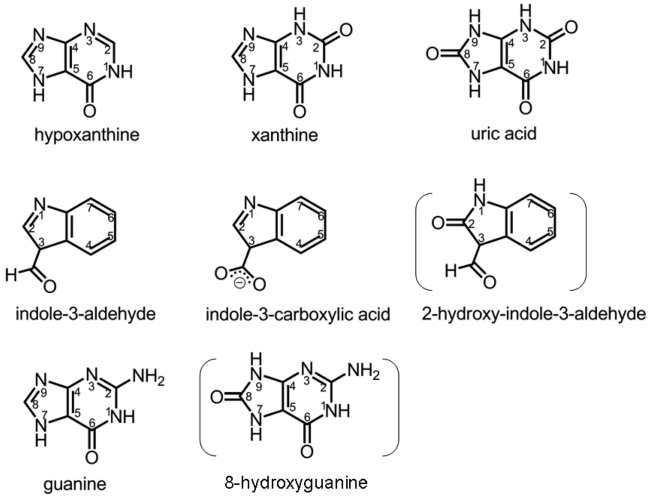

Figure 2. Chemical structures and numbering scheme of compounds used in this work.

Purification of Bovine Xanthine Oxidase. Bovine xanthine oxidase was purified from fresh, unpasteurized bovine milk (Scott Brothers Dairy, Chino, CA) as described elsewhere.[20] To eliminate possible problems caused by genetic heterogeneity in the dairy herd, the enzyme used for crystallographic work was isolated from milk obtained from an individual cow. The purified enzyme exhibited a ratio of absorbance at 280 and 450 nm of 6.0−6.8 and a percentage of functionality of 30−60% due to variability in the amount of the nonfunctional desulfo form of the enzyme present (in which a catalytically essential Mo=S group has been replaced by a second Mo=O group in the molybdenum coordination sphere). The percentage of functionality was determined as described previously by Massey and Edmondson.[21] A folate affinity column procedure[22] was used as a final purification step to enrich the functionality to >80%. The purified enzyme was made 1.0 mM in sodium salicylate and stored in liquid nitrogen and passed down a Sephadex G-25 column (to remove salicylate) prior to being used.

Crystallization, Data Acquisition, and Structure Determination. Xanthine oxidase crystals were grown using the batch method according to previously published methods using microbridges to hold batch solutions in sealed wells of a 24-well tray.[11,19] The batch solutions consisted of 10 μL of a 34.5 μM (5 mg/mL) enzyme solution mixed with 5 or 6 μL of a 12% PEG 8000 precipitant solution. Throughout this work, the enzyme concentration refers to the total monomer

concentration based on an extinction coefficient at 450 nm of 37.8 mM^{-1} cm^{-1}.[20]

Crystals were grown in the dark at 25 °C for 2−3 days before being harvested. A 42% solution of PEG 200 was used as a cryoprotectant. Indole-3-acetaldehyde or guanine was introduced to xanthine oxidase crystals via soaking to reach a final substrate concentration of 1 mM in the crystal well. After soaking in indole-3-acetaldehyde for 2−5 min or soaking in guanine for 5−8 min, crystals were mounted and flash-frozen in liquid nitrogen. Diffraction data were collected at Argonne National Laboratory on the LRL-CAT beamline using a wavelength of 0.9793 Å and a MARCCD 165 detector. Data sets were collected to a resolution of 1.6 Å for both structures reported here.

Crystallographic data were processed using the MOSFLM package of the CCP4 program suite.[23] The structure of each complex was determined by molecular replacement using the MOLREP package of CCP4 with the previously reported crystal structure of xanthine oxidase of Enroth et al. as the search model [Protein Data Bank (PDB) entry 1FIQ[5]]. The output structure was refined first by rigid body refinement and subsequently by restrained refinement using the REFMAC program of the CCP4 suite.[24−28] The weighting term for geometric restraints was adjusted in REFMAC to minimize R_{cryst} while at the same time minimizing the difference between R_{cryst} and R_{free}. No noncrystallographic symmetry restraints were used during refinement of the structures. Water molecules were added to both the crystal structures (using REFMAC) prior to building in the substrates.

Structure files for indole-3-acetaldehyde and guanine were constructed using the PRODRG2 server,[29] and the respective Protein Data Bank entries were built into the corresponding $2F_0 - F_c$ and $F_0 - F_c$ omit electron density maps observed in the active sites using COOT.[30] After the substrate structure files had been merged with those for the refined protein structures, the results were refined again using the restrained refinement mode in REFMAC. The final structure files were deposited into the PDB as entries 3NVZ and 3NVW for the structures of xanthine oxidase in complex with indole-3-acetaldehyde and guanine, respectively. All structures in the figures have been rendered using PyMol.[31]

UV−Visible Spectroscopic Analysis of Products of Hydroxylation of Indole-3-acetaldehyde by Bovine Xanthine Oxidase. To confirm the product of hydroxylation of indole-3-acetaldehyde by bovine xanthine oxidase as the corresponding carboxylic acid, the following experiments were performed. With the bovine enzyme, which was effective, 50 μM indole-3-acetaldehyde was incubated aerobically with a catalytic amount (118 nM) of enzyme in 1 mL of 0.1 M sodium pyrophosphate, 0.3 mM EDTA buffer (pH 8.5) at 4 °C in the dark for 24 h. The UV−visible absorption spectrum of the reaction product was recorded directly and was corrected for the relatively small absorbance due to the enzyme. The UV−visible absorption spectrum of the eluate was then recorded, and the dominant hydroxylation product of indole-3-acetaldehyde was identified as indole-3-carboxylic acid based on a comparison of the observed UV−vis spectra of the reaction products with that authentic indole-3-carboxylic acid.

Reductive Half-Reaction Experiments. Rapid kinetic experiments with indole-3-acetaldehyde were performed using an Applied Photophysics SX-18MV stopped-flow instrument equipped with a diode array detector. Enzyme solutions in glass tonometers were made anaerobic by alternately evacuating and flushing with O_2-scrubbed argon over the course of ≥1 h. Substrate solutions were made anaerobic by being bubbled with argon in airtight glass syringes for 10−15 min. The reaction conditions included 0.1 M pyrophosphate and 0.3 mM EDTA (pH 8.5) at 25 °C. Reactions were followed at 450 nm, monitoring the decrease in absorbance due to enzyme reduction. The initial reaction mix typically contained ∼4 μM functional enzyme and 25−500 μM substrate (after mixing). For each substrate concentration used, the reaction was repeated in triplicate with kinetic transients fit to a single-exponential equation using manufacturer's software to obtain k_{obs} values, which were then averaged for each substrate concentration. The kinetic parameters k_{red} and K_d were obtained from hyperbolic fits to plots of k_{obs} versus [S] using eq 1:

$$k_{obs} = (k_{red}[S])/(K_d + [S]) \quad (1)$$

RESULTS

Crystal Structure of Xanthine Oxidase in Complex with Indole-3-acetaldehyde. The crystal structure of xanthine oxidase in complex with indole-3-acetaldehyde was determined at 1.6 Å resolution by molecular replacement using the previously reported crystal structure of xanthine oxidase of Enroth et al. as the search model (PDB entry 1FIQ[5]). Final R factors were an R_{cryst} of 21.5% and an R_{free} of 24.6% (Table 1).

Table 1. Statistics for Data Collection and Refinement of the Crystal Structures of Xanthine Oxidase in Complex with Indole-3-acetaldehyde and Guanine

	XO with indole-3-acetaldehyde	XO with guanine
PDB entry	3NVZ	3NVW
space group	$P2_1$	$P2_1$
cell dimensions		
a, *b*, *c* (Å)	133.4, 73.7, 138.9	132.7, 73.4, 138.1
α, *β*, *γ* (deg)	90.0, 97.1, 90.0	90.0, 97.0, 90.0
resolution (Å)	45.2−1.6	131.7−1.6
wavelength (Å)	0.9793	0.9793
no. of unique reflections (test set)	339741 (17094)	334928 (16908)
completeness (%) [highest-resolution shell (Å)]	96.5 (93.3)	96.6 (94.3)
I/σ[a] (highest-resolution shell)	6.1 (2.2)	18.2 (2.4)
R_{cryst} (highest-resolution shell)	21.5 (37.9)	18.4 (23.8)
R_{free} (highest-resolution shell)	24.6 (44.3)	21.2 (26.8)
Ramachandran statistics[b] (%)	90.4, 9.0, 0.3, 0.3	90.0, 9.7, 0.1, 0.2
mean coordinate error based on the free *R* value (Å)	0.103	0.091
mean coordinate error based on the maximum likelihood (Å)	0.076	0.059
root-mean-square deviation for bond lengths (Å)	0.011	0.008
root-mean-square deviation for bond angles (deg)	1.3	1.2
average *B* value (Å^2)	21.6	18.0
no. of non-hydrogen atoms in refinement	20672	21495
no. of waters	1600	2173

[a] I/σ is defined as the ratio of the averaged value of the intensity to its standard deviation. [b] Ramachandran statistics indicate the percentage of residues in the most favored, additionally allowed, generously allowed, and disallowed regions of the Ramachandran diagram as defined by PROCHECK.[34]

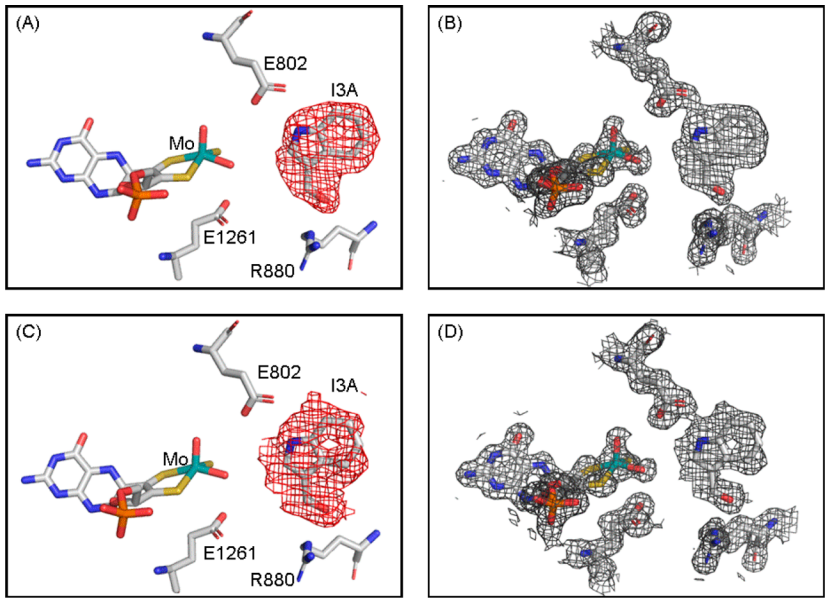

Figure 3. Electron density maps of xanthine oxidase complexed with indole-3-acetaldehyde. Both active sites of the assymmetric unit (A and B, and C and D) have the same single dominant orientation with C-2 proximal to the molybdenum center. Panels A and C show $F_0 - F_c$ omit maps contoured at 3.0σ, while panels B and D show $2F_0 - F_c$ omit maps contoured at 1.0σ, all within 2.0 Å of all atoms shown. All omit maps were constructed prior to addition of indole-3-acetaldehyde in the refinement model and subsequently overlaid with the final model. The atoms were color-coded as follows: cyan for molybdenum, white for carbon, blue for nitrogen, red for oxygen, yellow for sulfur, and orange for phosphorus. All structures were rendered with PyMOL.[31] Abbreviation: I3A, indole-3-acetaldehyde.

There was a single homodimer in the asymmetric unit, with an overall structure very similar to that seen previously for the oxidized bovine enzyme[5] and our own previously reported structures of the enzyme in complex with 2-hydroxy-6-methylpurine, xanthine, lumazine, and hypoxanthine,[11,17,19] including the observation of finite electron density for the C-terminal residues (residues 1316−1325) of one monomer of the homodimer, and these were included during the refinement process.

Figure 3 shows $F_0 - F_c$ and $2F_0 - F_c$ omit electron density maps for indole-3-acetaldehyde bound in each of the two active sites in the asymmetric unit, contoured at 3.0σ and 1.0σ, respectively. In each active site, a single dominant orientation of indole-3-acetaldehyde is observed. The aromatic indole ring is sandwiched between phenylalanine residues Phe 1009 and Phe 914 (Figure 4), with the indole nitrogen within hydrogen bonding distance of Glu 802 (at 2.78 and 2.86 Å in the two active sites) and the exocyclic carbonyl oxygen within hydrogen bonding distance of Arg 880 (2.89 and 3.15 Å from the two guanidinium nitrogens in one active site and 2.99 and 3.36 Å in the other). C-2 of the substrate is within 3.96 Å (and 4.07 Å) of the equatorial oxygen of the Mo-OH group and 5.76 Å (and 5.97 Å) of the molybdenum. No bridging electron density is observed between the equatorial Mo-OH group and the proximal carbon of the substrate, indicating that catalysis has not progressed to any significant degree in either active site of the asymmetric unit, presumably because of the low reactivity of the substrate.

It is evident from the crystal structure that the substrate is not optimally oriented for hydroxylation of the exocyclic carbonyl group, whose carbon is some 5.4 Å from the oxygen of the Mo-OH group. Arg 880 appears to be principally responsible for the unfavorable orientation, because of its interaction with the exocyclic aldehyde group, and it is noteworthy that this residue is not conserved in the otherwise very similar vertebrate aldehyde oxidases (where a methionine is most commonly found at the corresponding position[32]). To become hydroxylated, as observed experimentally (see below), it is necessary that the indole-3-aldehyde rotate within the plane defined by the two phenylalanine residues by some 30°, a motion that disrupts the interaction between the aldehyde functionality of the substrate and Arg 880 (Figure 4) but is otherwise minimally restricted from a steric standpoint. Although not quantified directly in this study, we note that the energetics of this motion must be small compared to kT at room temperature because the indole-3-aldehyde is in fact experimentally observed to be hydroxylated.

While the two phenylalanines of the active site constrain the substrate to a plane approximately perpendicular to the base plane of the molybdenum coordination sphere, the substrate can assume multiple orientations within this plane. We have previously observed, for example, two alternate orientations for both hypoxanthine and 6-mercaptopurine binding in bovine xanthine oxidase,[19] with one orientation being appropriate for hydroxylation and the other not, having the site of hydroxylation (C-2) oriented away from the molybdenum center rather than toward it. More generally, for any given substrate, an equilibrium distribution of orientations may be considered to exist with a distribution of intrinsic reactivities, in which case the overall catalytic throughput would reflect the weighted average of the catalysis for the ensemble of substrate orientations, the individual contribution of each being determined by the product of its fractional population in a given orientation and its intrinsic catalytic rate, as given in eq 2.

$$k_{red} = \sum_n (q_i k_i) \quad (2)$$

where k_{red} is the rate constant for enzyme reduction, q_i is the fractional population of orientation i, and k_i is the intrinsic catalytic rate for orientation i. The situation is an example of the principal of near-attack conformers, in which thermally

dx.doi.org/10.1021/bi401465u | *Biochemistry* 2014, 53, 533−541

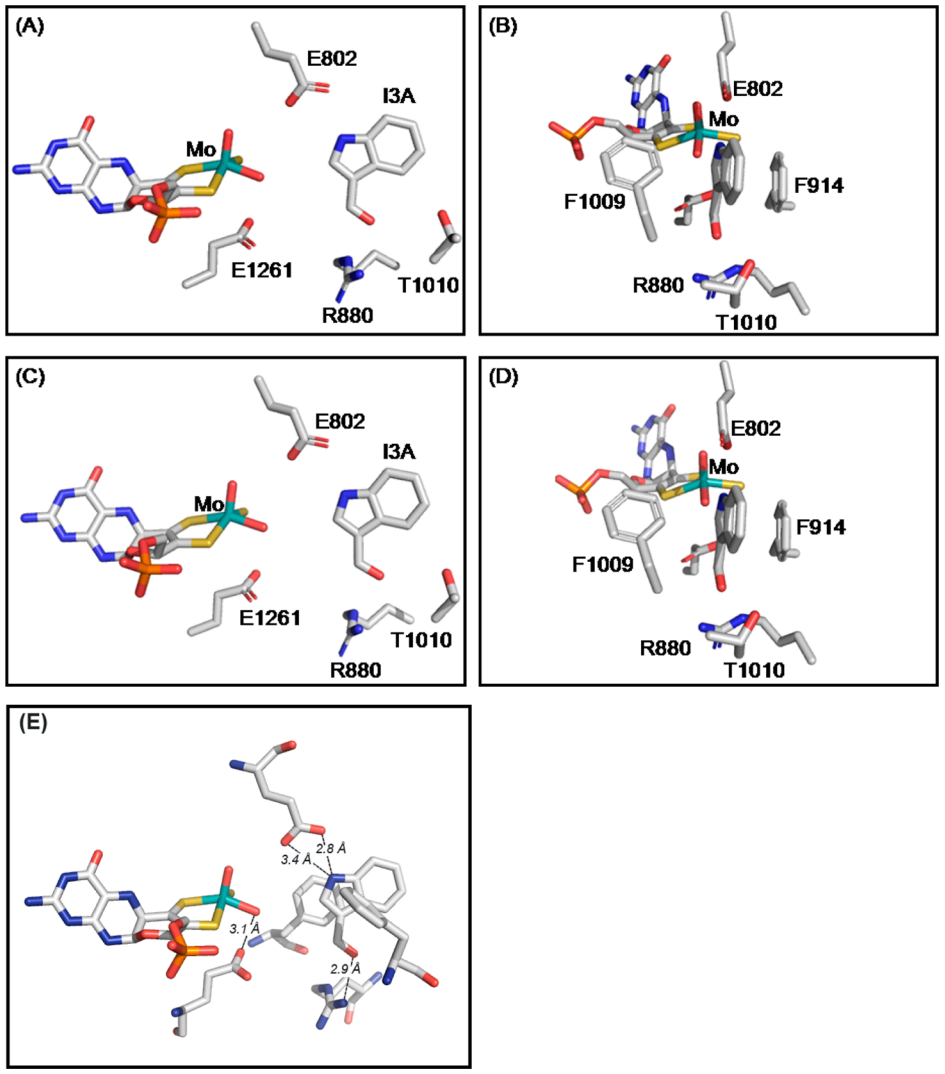

Figure 4. Structures of xanthine oxidase complexed with indole-3-acetaldehyde. Panels A and B show one active site, while panels C and D show the other active site in the asymmetric unit. Panels B and D are rotated approximately 90° about the vertical from panels A and C. Atoms are colored as in Figure 3. (E) Indole-3-acetaldehyde bound in the active site with Phe 914 and Phe 1009 shown, with the hydrogen bonding distances indicated. All structures were rendered with PyMOL.[31]

populated configurations of the Michaelis complex play an important role in facilitating the transition state and accelerating the reaction rate.[33−35] At the extreme limit, a strictly nonproductive orientation (k_i = 0) will have zero contribution to the overall rate of enzyme reduction. In the case of hypoxanthine,[15,19] the nonproductive orientation observed in the crystal structure represents an extreme case of this situation, having the wrong carbon (C-8 rather than C-2) oriented toward the molybdenum center for hydroxylation to yield xanthine (the known physiological product). The lack of reactivity of this orientation has been confirmed by the failure to detect the expected 6,8-dihydroxypurine product in the course of the reaction of the enzyme with hypoxanthine.[19] In the crystal structure with bound indole-3-acetaldehyde presented here, the observed orientation of the substrate suggests a single dominant but nonproductive orientation with C-2 proximal to the molybdenum center for hydroxylation, consistent with the observed low reactivity of the enzyme toward this substrate (see below).

Analysis of the Products of Hydroxylation of Indole-3-acetaldehyde by Bovine Xanthine Oxidase. The reactivity of indole-3-acetaldehyde as a substrate was next examined. The bovine enzyme is reported to slowly hydroxylate indole-3-acetaldehyde to the corresponding carboxylic acid (a reaction analogous to that of the *bona fide* molybdenum-containing aldehyde oxidase in plants that catalyzes the synthesis of this plant hormone under physiological conditions), which is confirmed here, the crystallographically observed orientation notwithstanding. Figure 5 shows the UV−visible absorption spectra of indole-3-acetaldehyde, authentic indole-3-carboxylic acid, and the product of hydroxylation of indole-3-acetaldehyde by the enzyme. It is clear that the UV−visible spectra of indole-3-acetaldehyde and indole-3-carboxylic acid are distinct, with local maxima at 244, 260, and 300 nm for the former and 278 nm for the latter. The product of the reaction of indole-3-acetaldehyde with xanthine oxidase has a normalized spectrum identical to that of authentic indole-3-carboxylic acid. We conclude that bovine xanthine oxidase is indeed able to hydroxylate indole-3-acetaldehyde and that the product of the reaction is indole-3-carboxylic acid.

Reductive Half-Reaction Experiments with Indole-3-acetaldehyde. In the orientation of indole-3-acetaldehyde

dx.doi.org/10.1021/bi401465u | *Biochemistry* 2014, 53, 533−541

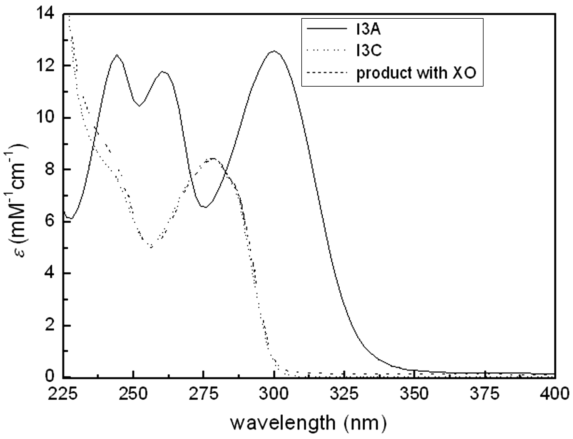

Figure 5. UV−visible absorption spectra of indole-3-acetaldehyde, indole-3-carboxylic acid, and the products of hydroxylation of indole-3-acetaldehyde by bovine xanthine oxidase. Spectra shown are for indole-3-acetaldehyde, indole-3-carboxylic acid, and the product of the reaction of indole-3-acetaldehyde with xanthine oxidase. The extinction coefficients of the reaction products are normalized at 278 nm where the local maximum is observed for the characteristic UV−vis absorption spectrum of indole-3-carboxylic acid. For the reaction with bovine xanthine oxidase, 118 nM enzyme was added prior to incubation for 1 day, and its absorption was subtracted as the baseline from that of the final reaction mix. Abbreviations: XO, xanthine oxidase; XDH, xanthine dehydrogenase; WT, wild type; I3A, indole-3-acetaldehyde; I3C, indole-3-carboxylic acid.

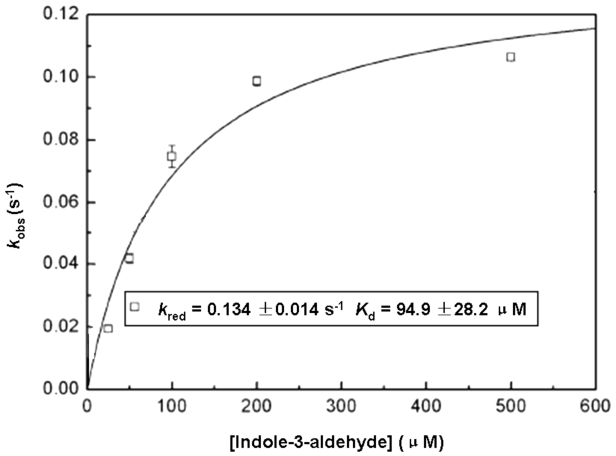

Figure 6. Plot of k_{obs} vs indole-3-acetaldehyde concentration for the reaction with xanthine oxidase. The reaction conditions included 0.1 M pyrophosphate buffer, 0.3 mM EDTA, pH 8.5, and 25 °C. The hyperbolic fit to the data indicated yields a k_{red} of 0.13 s^{-1} and a K_d of 95 μM.

seen crystallographically with the bovine enzyme, hydroxylation should occur at C-2 of the indole ring rather than the exocyclic carbonyl, which we observed experimentally as described above. Given the low intrinsic reactivity of xanthine oxidase toward indole-3-acetaldehyde and the inherent uncertainty in steady-state assays, to quantify the reactivity of the enzyme with indole-3-acetaldehyde we have undertaken a reductive half-reaction analysis rather than conventional steady-state experiments. The experiment involves mixing the oxidized enzyme with varying concentrations of indole-3-acetaldehyde, yielding a rate constant for enzyme reduction from the observed exponential decrease in absorbance as the substrate reduces the enzyme (see Experimental Procedures). Figure 6 shows a plot of the observed rate constant for reduction of xanthine oxidase under anaerobic conditions by varying concentrations of indole-3-acetaldehyde (following the loss of absorbance at 450 nm due to reduction of the enzyme's FAD and iron−sulfur centers). A hyperbolic fit to the data yields a limiting k_{red} of 0.13 s^{-1} and a K_d of 95 μM. It is evident that enzyme is compromised in terms of transition-state stabilization (k_{red} is less than 1% of the value of 18 s^{-1} observed with xanthine as the substrate[36]) but that the affinity of the enzyme for the substrate is decreased by a factor of only 6 (K_d for xanthine under the reaction conditions of 15 μM).

Given that indole-3-acetate is the sole product of the enzyme-catalyzed reaction, it is evident that the substrate aldehyde is able to reorient in the active site to bring the aldehyde group into the proximity of the molybdenum center for reaction to occur. This involves an ~30° rotation of the indole ring between the two active site phenylalanine residues Phe 914 and Phe 1009 of the bovine enzyme, a motion that appears to be sterically allowed on the basis of the crystal structure (Figure 4), if thermodynamically unfavorably in that it ruptures the hydrogen bond with Arg 880.

Crystal Structure of Xanthine Oxidase in Complex with Guanine. The overall protein structure of guanine-complexed xanthine oxidase at 1.6 Å resolution is again very similar to that previously reported for the oxidized enzyme, with all differences limited to the active site. Table 1 summarizes the structural refinement statistics, and Figure 7 shows the two active sites of the asymmetric unit overlaid with the $F_0 - F_c$ omit map contoured at 3σ and the $2F_0 - F_c$ omit map contoured at 1σ (with guanine omitted from the latter map). The strong positive electron density in the $F_0 - F_c$ omit map in each active site of the enzyme clearly indicates a single dominant orientation for the bound guanine with C-8 pointing away from and the C-2 amino group oriented toward the active site molybdenum center. Again, no electron density is observed connecting the Mo-OH group and guanine that might suggest partial progression through the catalytic sequence.

The interactions stabilizing the observed orientation of guanine include an approximately planar hydrogen bonding network involving the C-2 amino group of guanine with the side chain carboxylate group of Glu 802 (at 2.78 and 2.84 Å in the two active sites) and the Mo-OH oxygen (2.74 and 2.78 Å); Glu 1261 remains within hydrogen bonding distance of the Mo-OH group (at 3.11 and 3.06 Å, respectively) but does not interact directly with bound guanine in either active site of the asymmetric unit. The C-6 keto group are also within hydrogen bonding distance of the guanidinium group of Arg 880 (3.11 and 3.10 Å, respectively), and N-3 is within hydrogen bonding distance of Glu 802 (2.72 and 2.74 Å, respectively). This network is shown in Figure 7E, with the distances indicated. The two active site phenylalanine residues are again in van der Waals contact with the bound guanine (but are shown only in Figure 7E for the sake of clarity). The complex strongly resembles that seen with hypoxanthine that leads to hydroxylation at C-2 with that substrate,[15,19] but which is impossible with guanine given the presence of the C-2 amino group. The orientation of guanine is the opposite of that required for hydroxylation of C-8 of guanine. This unfavorable orientation, with the substrate misoriented by ~180°, is undoubtedly a major reason for the lack of reactivity of the enzyme toward guanine.

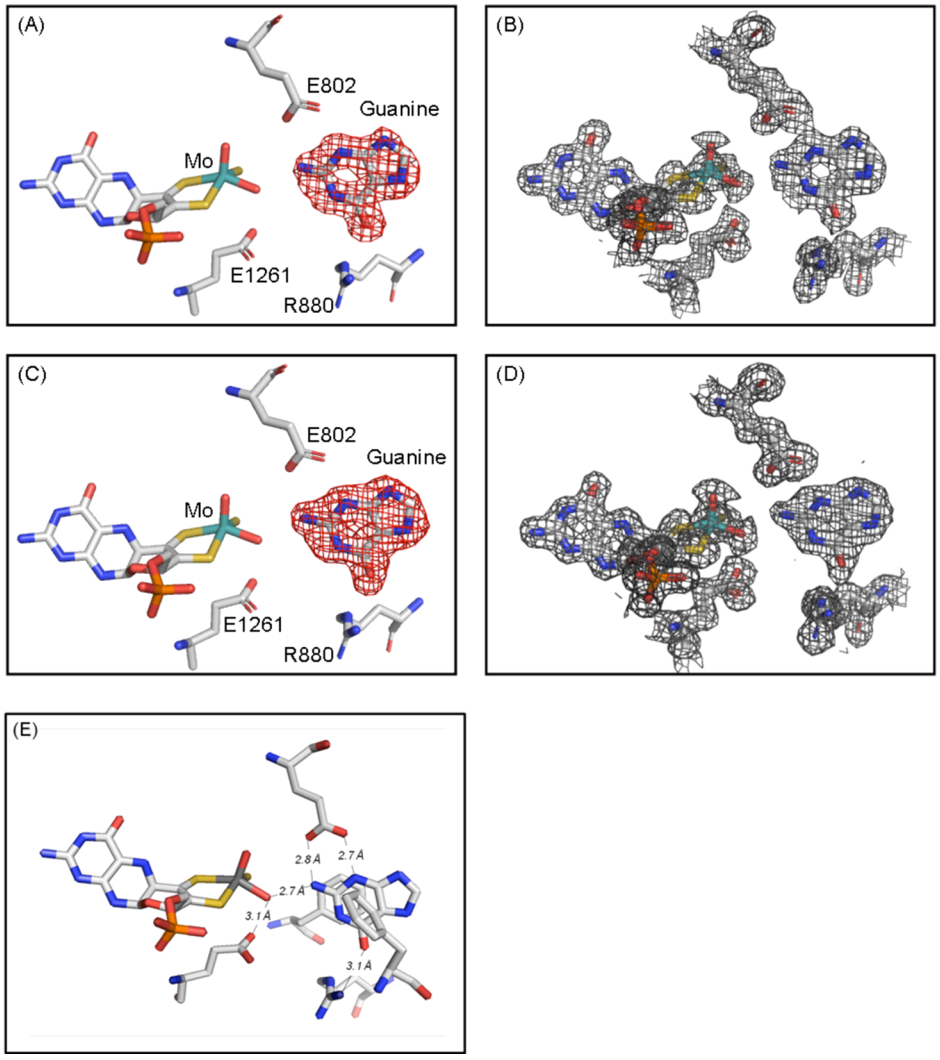

Figure 7. Structures of xanthine oxidase complexed with guanine. Panels A and B show one active site, while panels C and D show the other active site in the asymmetric unit. Panels A and C show $F_0 - F_c$ omit maps contoured at 3.0σ, and panels B and D show $2F_0 - F_c$ omit maps contoured at 1.0σ, all within 1.8 Å of all atoms shown. All the omit maps were constructed before the introduction of guanine for the refinement of the model and overlaid with the final model. Molybdenum is colored teal, carbon white, nitrogen blue, oxygen red, sulfur yellow, and phosphorus orange. (E) Guanine bound in the active site with Phe 914 and Phe 1009 shown, with the hydrogen bonding distances indicated. All structures were rendered with PyMOL.[31]

Even if guanine were able to transiently adopt a more favorable orientation (as indole-3-acetaldehyde is apparently able to do), the less effective stabilization of negative charge on the heterocycle in the course of the reaction due to the presence of the C-2 amino group substitution might well reduce the intrinsic susceptibility of the guanine C-8 to nucleophilic attack.[19] To quantitatively assess this effect, we have performed partial charge calculations for the neutral form of stable N-7-H tautomers of guanine and xanthine using the MOPAC 2009 software package.[37] We find that the positive partial charges at C-8 of guanine and xanthine are 0.026 and 0.065, respectively, and the partial charges on the C-8-H groups are 0.256 and 0.199, respectively. These results indicate that the overall polarity of the C-8-H bond and its susceptibility to nucleophilic attack is somewhat greater in xanthine that in guanine, but not sufficiently so to account for the vast difference in reactivity. We conclude that the unfavorable orientation guanine assumes upon binding to the enzyme is a principal reason it fails to serve as an effective substrate for xanthine oxidase.

DISCUSSION

In this work, we observe a single dominant orientation for binding of both indole-3-acetaldehyde and guanine in the active site of bovine xanthine oxidase, both of which are expected to be catalytically unproductive on the basis of the distance of the site to be hydroxylated from the catalytically labile equatorial Mo-OH group of the enzyme's molybdenum center. In the case of indole-3-acetaldehyde, while the substrate is readily accommodated between Phe 914 and Phe 1009 that define the substrate binding pocket, Arg 880 forms hydrogen bonds to the exocyclic aldehyde group that is hydroxylated in such a way that the carbonyl carbon is held approximately 5.4 Å from the oxygen of the Mo-OH group. To orient more appropriately for catalysis, the substrate must rotate some 30° to bring the exocyclic carbonyl into juxtaposition with the Mo-OH group. This is a relatively modest rearrangement, and the motion appears to be readily allowed sterically in the active site; although it involves disruption of the hydrogen bond with Arg 880, the hydrogen bond with Glu 802 is maintained (as are the

dx.doi.org/10.1021/bi401465u | *Biochemistry* 2014, 53, 533−541

hydrophobic contacts with Phe 914 and Phe 1009). It is likely that kT is sufficient to populate the catalytically effective orientation at least a portion of the time, in which case the situation is equivalent to the near-attack conformer formalism developed by Hur and Bruice,[33−35] which explicitly considers the majority of catalytic throughput occurring through configurations in the Michaelis complex that may lie far from the equilibrium mean. Such an interpretation is consistent with the small but finite value seen for k_{red} with indole-3-acetaldehyde (0.13 s^{-1}).

In the case of the complex of the enzyme with guanine, a catalytically ineffective orientation is again observed in the crystal structure, with the C-8 position that might otherwise become hydroxylated oriented essentially directly away from the Mo-OH group. The principal interactions that hold guanine in this unfavorable orientation are with Glu 802 (interacting with N3 and the C-2 amino group) and Arg 880, hydrogen bonding to the C-6 keto group. A rotation of guanine between the two phenylalanines of ∼180° is required to juxtapose its C-8 position with the molybdenum center, so large a rotation is sterically prevented by Glu 802 and Arg 880, both of which would have to move considerably to accommodate such a rotation. Although a computational analysis indicates that the C-8 position of guanine is indeed somewhat less reactive than that of xanthine, it appears that it is the orientation of guanine when bound to the enzyme that is the principal factor that allows the enzyme to discriminate against this potential substrate, preventing formation of the mutagenic 8-hydroxyguanine.

AUTHOR INFORMATION

Corresponding Author

*University of California, 1463 Boyce Hall, Riverside, CA 92521. E-mail: russ.hille@ucr.edu. Telephone: (951) 827-6354. Fax: (951) 827-2364.

Present Address

[†]H.C.: Department of Biochemistry and Cell Biology, Rice University, Houston, TX 77251-1892.

Funding

This work was supported by the U.S. Department of Energy (DE-SC0010666).

Notes

The authors declare no competing financial interest.

ACKNOWLEDGMENTS

We thank Dr. Takeshi Nishino for advice in use of the folate column procedure and for helpful discussions. Use of the Advanced Photon Source at Argonne National Laboratory was supported by the U.S. Department of Energy, Office of Science, Office of Basic Energy Sciences, under Contract DE-AC02-06CH11357. Use of the Lilly Research Laboratory Collaborative Access Team (LRL-CAT) beamline at Sector 31 of the Advanced Photon Source was provided by Eli Lilly & Co., which operates the facility.

REFERENCES

(1) Hille, R. (1996) The mononuclear molybdenum enzymes. *Chem. Rev. 96*, 2757−2816.

(2) Hille, R. (2002) Molybdenum and tungsten in biology. *Trends Biochem. Sci. 27*, 360−367.

(3) Hille, R. (2005) Molybdenum-containing hydroxylases. *Arch. Biochem. Biophys. 433*, 107−116.

(4) Hille, R., Nishino, T., and Bittner, F. (2011) Molybdenum enzymes in higher organisms. *Coord. Chem. Rev. 255*, 1179−1205.

(5) Enroth, C., Eger, B. T., Okamoto, K., Nishino, T., and Pai, E. F. (2000) Crystal structures of bovine milk xanthine dehydrogenase and xanthine oxidase: Structure-based mechanism of conversion. *Proc. Natl. Acad. Sci. U.S.A. 97*, 10723−10728.

(6) Leimkuhler, S., Stockert, A. L., Igarashi, K., Nishino, T., and Hille, R. (2004) The role of active site glutamate residues in catalysis of *Rhodobacter capsulatus* xanthine dehydrogenase. *J. Biol. Chem. 279*, 40437−40444.

(7) Huber, R., Hof, P., Duarte, R. O., Moura, J. J. G., Moura, I., Liu, M. Y., LeGall, J., Hille, R., Archer, M., and Romao, M. J. (1996) A structure-based catalytic mechanism for the xanthine oxidase family of molybdenum enzymes. *Proc. Natl. Acad. Sci. U.S.A. 93*, 8846−8851.

(8) Stockert, A. L., Shinde, S. S., Anderson, R. F., and Hille, R. (2002) The reaction mechanism of xanthine oxidase: Evidence for two-electron chemistry rather than sequential one-electron steps. *J. Am. Chem. Soc. 124*, 14554−14555.

(9) Hille, R., and Sprecher, H. (1987) On the mechanism of xanthine-oxidase: Evidence in support of an oxo transfer mechanism in molybdenum-containing hydroxylases. *J. Biol. Chem. 262*, 10914−10917.

(10) McWhirter, R. B., and Hille, R. (1991) The reductive half-reaction of xanthine-oxidase: Identification of spectral intermediates in the hydroxylation of 2-hydroxy-6-methylpurine. *J. Biol. Chem. 266*, 23724−23731.

(11) Pauff, J. M., Zhang, J. J., Bell, C. E., and Hille, R. (2008) Substrate orientation in xanthine oxidase: Crystal structure of enzyme in reaction with 2-hydroxy-6-methylpurine. *J. Biol. Chem. 283*, 4818−4824.

(12) Kim, J. H., Ryan, M. G., Knaut, H., and Hille, R. (1996) The reductive half-reaction of xanthine oxidase: The involvement of prototropic equilibria in the course of the catalytic sequence. *J. Biol. Chem. 271*, 6771−6780.

(13) Xia, M., Dempski, R., and Hille, R. (1999) The reductive half-reaction of xanthine oxidase: Reaction with aldehyde substrates and identification of the catalytically labile oxygen. *J. Biol. Chem. 274*, 3323−3330.

(14) Cao, H. N., Pauff, J., and Hille, R. (2011) Substrate orientation and the origin of catalytic power in xanthine oxidoreductase. *Indian J. Chem., Sect. A: Inorg., Bio-inorg., Phys., Theor. Anal. Chem. 50*, 355−362.

(15) Dietzel, U., Kuper, J., Doebbler, J. A., Schulte, A., Truglio, J. J., Leimkuhler, S., and Kisker, C. (2009) Mechanism of Substrate and Inhibitor Binding of *Rhodobacter capsulatus* Xanthine Dehydrogenase. *J. Biol. Chem. 284*, 8759−8767.

(16) Pauff, J. M., Hemann, C. F., Junemann, N., Leimkuhler, S., and Hille, R. (2007) The role of arginine 310 in catalysis and substrate specificity in xanthine dehydrogenase from *Rhodobacter capsulatus*. *J. Biol. Chem. 282*, 12785−12790.

(17) Pauff, J. M., Cao, H., and Hille, R. (2009) Substrate orientation and catalysis at the molybdenum site in xanthine oxidase crystal structures in complex with xanthine and lumazine. *J. Biol. Chem. 284*, 8751−8758.

(18) Yamaguchi, Y., Matsumura, T., Ichida, K., Okamoto, K., and Nishino, T. (2007) Human xanthine oxidase changes its substrate specificity to aldehyde oxidase type upon mutation of amino acid residues in the active site: Roles of active site residues in binding and activation of purine substrate. *J. Biochem. 141*, 513−524.

(19) Cao, H., Pauff, J. M., and Hille, R. (2010) Substrate orientation and catalytic specificity in the action of xanthine oxidase: The sequential hydroxylation of hypoxanthine to uric acid. *J. Biol. Chem. 285*, 28044−28053.

(20) Massey, V., Brumby, P. E., and Komai, H. (1969) Studies on milk xanthine oxidase: Some spectral and kinetic properties. *J. Biol. Chem. 244*, 1682.

(21) Edmondso, D., Ballou, D., Vanheuve, A., Palmer, G., and Massey, V. (1973) Kinetic studies on substrate reduction of xanthine-oxidase. *J. Biol. Chem. 248*, 6135−6144.

(22) Nishino, T., and Tsushima, K. (1981) Purification of highly-active milk xanthine-oxidase by affinity-chromatography on sepharose 4B-folate gel. *FEBS Lett. 131*, 369−372.
(23) Potterton, E., Briggs, P., Turkenburg, M., and Dodson, E. (2003) A graphical user interface to the CCP4 program suite. *Acta Crystallogr. D59*, 1131−1137.
(24) Turkenburg, J. P., and Dodson, E. J. (1996) Modern developments in molecular replacement. *Curr. Opin. Struct. Biol. 6*, 604−610.
(25) Murshudov, G. N., Vagin, A. A., and Dodson, E. J. (1997) Refinement of macromolecular structures by the maximum-likelihood method. *Acta Crystallogr. D53*, 240−255.
(26) Pannu, N. S., Murshudov, G. N., Dodson, E. J., and Read, R. J. (1998) Incorporation of prior phase information strengthens maximum-likelihood structure refinement. *Acta Crystallogr. D54*, 1285−1294.
(27) Murshudov, G. N., Vagin, A. A., Lebedev, A., Wilson, K. S., and Dodson, E. J. (1999) Efficient anisotropic refinement of macromolecular structures using FFT. *Acta Crystallogr. D55*, 247−255.
(28) Winn, M. D., Ballard, C. C., Cowtan, K. D., Dodson, E. J., Emsley, P., Evans, P. R., Keegan, R. M., Krissinel, E. B., Leslie, A. G. W., McCoy, A., McNicholas, S. J., Murshudov, G. N., Pannu, N. S., Potterton, E. A., Powell, H. R., Read, R. J., Vagin, A., and Wilson, K. S. (2011) Overview of the CCP4 suite and current developments. *Acta Crystallogr. D67*, 235−242.
(29) Schuttelkopf, A. W., and van Aalten, D. M. F. (2004) PRODRG: A tool for high-throughput crystallography of protein-ligand complexes. *Acta Crystallogr. D60*, 1355−1363.
(30) Emsley, P., and Cowtan, K. (2004) Coot: Model-building tools for molecular graphics. *Acta Crystallogr. D60*, 2126−2132.
(31) DeLano, W. L. (2004) *The PyMol Molecular Graphics System*, DeLano Scientific LLC, San Carlos, CA.
(32) Coelho, C., Mahro, M., Trincao, J., Carvalho, A. T. P., Ramos, M. J., Terao, M., Garattini, E., Leimkuhler, S., and Romao, M. J. (2012) The First Mammalian Aldehyde Oxidase Crystal Structure: Insights into Substrate Specificity. *J. Biol. Chem. 287*, 40690−40702.
(33) Hur, S., and Bruice, T. C. (2002) The mechanism of catalysis of the chorismate to prephenate reaction by the *Escherichia coli* mutase enzyme. *Proc. Natl. Acad. Sci. U.S.A. 99*, 1176−1181.
(34) Hur, S., and Bruice, T. C. (2003) Comparison of formation of reactive conformers (NACs) for the Claisen rearrangement of chorismate to prephenate in water and in the *E. coli* mutase: The efficiency of the enzyme catalysis. *J. Am. Chem. Soc. 125*, 5964−5972.
(35) Hur, S., and Bruice, T. C. (2003) Enzymes do what is expected (chalcone isomerase versus chorismate mutase). *J. Am. Chem. Soc. 125*, 1472−1473.
(36) Olson, J. S., Ballou, D. P., Palmer, G., and Massey, V. (1974) Reaction of xanthine-oxidase with molecular oxygen. *J. Biol. Chem. 249*, 4350−4362.
(37) Stewart, J. J. P. (2008) *MOPAC 2009*, Stewart Computational Chemistry, Colorado Springs, CO.